Applied Catalysis B: Environmental 97 (2010) 248–256

Contents lists available at ScienceDirect

Applied Catalysis B: Environmental

journal homepage: www.elsevier.com/locate/apcatb

Hydrogenolysis of glycerol to propanediols over a Pt/ASA catalyst: The role of acid and metal sites on product selectivity and the reaction mechanism

I. Gandarias[a,*], P.L. Arias[a], J. Requies[a], M.B. Güemez[a], J.L.G. Fierro[b]

[a] School of Engineering (UPV/EHU), c/Alameda Urquijo s/n, 48013 Bilbao, Spain
[b] Institute of Catalysis and Petrochemistry, c/Marie Curie s/n, 28049 Madrid, Spain

ARTICLE INFO

Article history:
Received 18 January 2010
Received in revised form 26 March 2010
Accepted 10 April 2010
Available online 24 April 2010

Keywords:
Glycerol
Hydrogenolysis
Propanediol
Pt/ASA
Hydrogen spillover
Solid acid

ABSTRACT

Pt supported on amorphous silico alumina (Pt/ASA) was studied as a catalyst for glycerol hydrogenolysis (dehydration + hydrogenation) to 1,2-propanediol under mild operation conditions (493 K and 45 bar H_2 pressure). Glycerol hydrogenolysis also took place in experiments performed under N_2 pressure due to hydrogen available from glycerol aqueous phase reforming. As both acid and metallic sites are involved in this process a study including activity tests and different characterization techniques (TPR and FTIR of adsorbed pyridine, NH_3-TPD, XPS and TGA) were applied to this catalytic system (ASA support and Pt/ASA catalyst) in order to get a deeper understanding about their interactions.

1. Introduction

Nowadays large amounts of glycerol are generated as a by-product in biodiesel manufacture by transesterification of seed oils. Therefore, glycerol price experimented constant reduction during the last years, allowing new interesting applications like the production of high added value chemicals [1]. Among the different possible transformations of glycerol, the selective conversion to 1,2 and 1,3-propanediol (PDO), which are usually produced from petroleum derivates, presents a special interest [2]. 1,3-PDO is a starting material in the production of polytrimethylene terephthalate (PTT), which is used for the manufacture of fibers and resins [3], while 1,2-PDO is a commodity chemical widely used in the manufacture of a significant number of industrial and consumer products [4].

Propylene glycols can be produced through a two-step process: glycerol is first dehydrated to 1-hydroxypropan-2-one (acetol) and 3-hydroxypropanal (3-HPA), which are subsequently hydrogenated to 1,2- and 1,3-PDO respectively [5]. Various bi-functional metal-acid catalysts, which combine acid sites for dehydration reactions and metal sites for hydrogenation reactions, have been attempted for the conversion of glycerol to PDOs. Investigations on Pt [6], Ru [7], Ru + Re [8] and Rh [9] on different acid supports have been reported. The role of the acid function of the supports on glycerol hydrogenolysis with Cu catalysts has been also studied [10], even at ambient hydrogen pressure [11]. Miyazawa et al. developed an intense work with the aim to develop a Ru/C catalyst for glycerol hydrogenolysis in combination with an ion-exchange resin [12–14]. Besides dehydration and hydrogenation reactions, other unwanted side reactions such as cracking, addition and coking also occur simultaneously [10]. Scarce information has been reported about the role of acid and metallic sites, the acid–metal interaction, and H_2 availability effects on glycerol hydrogenolysis and side reactions. Accordingly, this work is focused on the hydrogenolysis of glycerol over Pt supported on an amorphous silica–alumina (Pt/ASA), analyzing the effect that the presence of Pt metallic sites and H_2 availability has on the catalyst performance. This will be discussed through the study of glycerol conversion, coke formation and selectivity to PDOs. The information regarding the structure of fresh and used catalysts was assessed using several physico-chemical techniques such as temperature-programmed reduction (TPR), FTIR spectroscopy of adsorbed pyridine, temperature-programmed desorption of ammonia (TPD-NH_3), X-ray photoelectron spectroscopy (XPS) and thermogravimetric analysis (TGA). All the data collected from the activity tests and catalysts characterization were utilized to gain a deeper understanding of this catalytic system and to formulate a reaction scheme of glycerol hydrogenolysis and degradation process.

* Corresponding author at: Escuela Técnica Superior de Ingeniería, Alameda Urquijo s/n, P.C. 48013 Bilbao, Spain. Tel.: +34 946017297; fax: +34 946014179.
E-mail address: inaki.gandarias@ehu.es (I. Gandarias).

0926-3373/$ – see front matter © 2010 Elsevier B.V. All rights reserved.
doi:10.1016/j.apcatb.2010.04.008

Table 1
Characteristics of the catalysts.

Sample	Pt (wt.%)[a]	Al_2O_3 (wt.%)[a]	Pretreatment	I_{1543}/I_{1452} ratio[d]
ASA	–	15.7	Degassing[b]	0.058
			Reduction[c]	0.060
Pt/ASA	0.7	15.1	Degassing[b]	0.056
			Reduction[c]	0.092

[a] Chemical composition determined by ICP.
[b] Samples were degassed at 723 K for 1 h.
[c] Samples were reduced in a H_2 flow at 673 K during 1 h and then degassed at 723 K for 1 h.
[d] As determined by FTIR of adsorbed pyridine.

2. Experimental

2.1. Catalyst

Amorphous silica–alumina (ASA) (surface area 389 m^2/g, pore volume 0.63 mL/g) and ASA loaded with 1 wt.% of Pt (1% Pt/ASA) were kindly supplied by Shell. Table 1 lists the Pt and Al content of the catalyst. Catalyst samples for activity tests were used in powdered form with granule size between 320 and 500 μm. They were used without further pretreatment.

2.2. Activity test

The reaction of glycerol hydrogenolysis was carried out in a 50 mL stainless steel autoclave with a magnetic stirrer, using 41 mL glycerol aqueous solution. The standard activity test was conducted under the following conditions: 493 K reaction temperature, 45 bar hydrogen or nitrogen pressure, 24 h reaction time, 20 wt.% glycerol aqueous solution, and 166 mg of catalysts/g of reactant (Pt/ASA or ASA). The stirring speed was set constant at 550 rpm. Reaction temperature and reacting atmosphere were changed to investigate the dependence of conversion and selectivities on the operating conditions. In addition, to elucidate the reaction mechanism of glycerol hydrogenolysis and degradation, 1,3-PDO, 1,2-PDO, ethylene glycol (EG), acetol, and 2-propanol were also used as reactants. The concentration of these reactants on the aqueous solution fed is described when the corresponding results are discussed.

In all experiments, 20.5 mL of deionized water and the catalyst powder (inside a basket) were placed in the autoclave; then the reactor was purged with N_2 (99.999% Air Liquide). After purging, the reactor was heated to the required temperature and the N_2 or H_2 (99.999% Air Liquide) pressure was increased up to 45 bar. The temperature was monitored with a thermocouple that was inserted into the autoclave and connected to the thermo-controller. 20.5 mL of the aqueous solution of the reactant, having twice the desired concentration, was placed on a feed cylinder and heated to the reaction temperature. Reaction starting time was established when the line connecting the feed cylinder and the reactor was opened. H_2 or N_2 pressure was kept constant during the reaction, keeping the reactor connected to a H_2 or N_2 flowing line with constant 45 bar pressure. Along the reaction seven liquid samples (1.2–1.7 mL each) were taken in order to obtain the time evolution of reactant and product concentrations. These compounds were analyzed using a gas chromatograph (Agilent Technologies, 7890 A) equipped with a flame ionization detector (FID) and a thermal conductivity detector (TCD). A Meta-Wax capillary column (diameter 0.53 mm, length 30 m) was used for separation. After the reaction, the gas phase products were collected in a gas bag and analyzed with another GC-TCD-FID (Agilent Technologies, 7890 A) equipped with a molecular sieve column (HP-MOLESIEVE, diameter 0.535 mm, length 30 m) and a capillary column (HP-PLOT/Q, diameter 0.320 mm, length 30 m). Liquid products were identified using GC–MS (Agilent Technologies, 5973). Conversion of the reactants in all reaction tests were calculated based on the following equation:

$$\text{Conversion of react. (\%)} = \frac{\text{sum of C-based mol of all liquid prod. } t = t}{\text{C-based mol of react. } t = 0}$$

The conversions calculated by this method were compared with the conversions defined as (reactant $t = 0$ – reactant $t = t$)/(reactant $t = 0$), in order to determine the error that is made when the gas products formed during the process are not accounted in the conversion calculations. Selectivities were only calculated for liquid products using the following equation:

$$\text{Selectivity of liquid products (\%)} = \frac{\text{C-based mol of the product}}{\text{Sum of C-based mol of all liquid products}}$$

The yield was calculated using the firstly defined conversion:

$$\text{Yield} = \frac{\text{conversion (\%)} \times \text{selectivity (\%)}}{100}$$

2.3. Characterization

Chemical analysis of the catalysts was performed by Inductively Coupled Plasma Atomic Emission (ICP-AES) using a Perkin-Elmer Optima 2000 instrument. The solid samples where treated with a mixture of HF, HCl and HNO_3 at 453 K in a microwave oven. The metal content of the catalysts is summarized in Table 1. Fresh Pt/ASA and ASA catalysts (not used in the activity test) were characterized by temperature-programmed reduction (TPR) and FTIR spectra of adsorbed pyridine.

Temperature-programmed reduction (TPR) experiments were carried out on a Micromeritics 3000 analyzer interfaced to a data station. A 50 mg catalyst sample was reduced in flowing gas containing 10 vol.% H_2 in Ar at a total flow rate of 50 mL min^{-1}, and using a heating rate of 15 K min^{-1} up to a final temperature of 1273 K. The FTIR spectra of adsorbed pyridine were recorded to determine the relative Brønsted and Lewis acidity of the reduced Pt/ASA and ASA catalysts. Self-supporting wafers of the oxide catalysts with a thickness of 10–12 mg cm^{-2} were prepared by pressing the powdered samples at a pressure of 7×10^3 kg cm^{-2} for 10 min. The wafer was introduced into an IR cell fitted with greaseless stopcocks and KBr windows. The samples were first purged in a helium flow at 673 K for 0.5 h. Some samples were reduced in a H_2 flow at 673 K for 1 h, prior to degassing at 723 K for 1 h. Subsequently, samples were contacted with approximately 2 mbar of pyridine and then degassed at 393 K for 1 h to remove the physisorbed pyridine.

The acidity of fresh and spent Pt/ASA and ASA catalysts was determined by ammonia temperature-programmed desorption (TPD) measurements carried out with the same apparatus described for TPR. After loading, a sample of 0.050 g was pretreated in a He (99.996%, Air Liquide) stream at 773 K for 0.5 h. Following this, the sample was cooled to 373 K and ammonia-saturated in a stream of 5% NH_3/He (Air Liquide) flow (50 mL min^{-1}) for 0.5 h. Then, after catalyst equilibration in a helium flow at 373 K for 0.5 h, the ammonia was desorbed using a linear heating rate of 10 K min^{-1} to 1123 K. In order to determine the total acidity of the catalyst from its NH_3 desorption profile, the area under the curve was integrated. A semiquantitative comparison of the strength distribution was achieved by Gaussian deconvolution of the peaks. Weak, medium and strong acidities were defined as the areas under the peaks at the lowest, medium and highest temperatures respectively.

X-ray photoelectron spectra were acquired with a VG Escalab 200R spectrometer equipped with a hemispherical electron analyzer and an Mg Kα ($h\nu = 1253.6$ eV) X-ray source. The energy regions of Al 2p, Si 2p, O 1s, C 1s and Pt $4d_{5/2}$ core levels for ASA and Pt/ASA fresh and spent samples were recorded. Although the most intense photoemission lines of platinum were those arising from the Pt 4f levels, this energy region was overshadowed by the presence of a very strong Al 2p peak, and thus the Pt 4d lines were

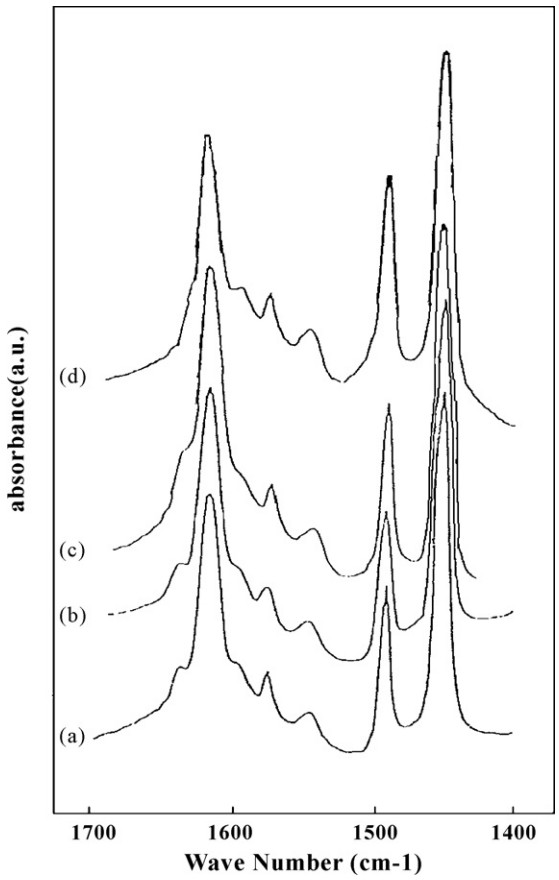

Fig. 1. FTIR spectra of pyridine chemisorbed on: (a) degassed ASA, (b) reduced ASA, (c) degassed Pt/ASA and (d) reduced Pt/ASA.

analyzed instead [15]. Peak intensities were estimated by calculating the integral of each peak after smoothing and subtraction of a Shirley background. Atomic surface contents were estimated from the areas of the peaks, corrected using the corresponding sensitivity factors [16].

Finally, the amount of coke deposited on the spent catalysts was determined with a thermogravimetric TGA/SDTA851^e equipment (Mettler Toledo), measuring the weight change in the coked catalysts during oxidation. The burning of coke was carried out by raising sample temperature to a final temperature of 1073 K at a rate of 10 K min^{-1} in a 20% O_2/N_2 mixture.

3. Results and discussion

3.1. The effect of Pt and H_2 on the acidity of ASA support

The IR spectra of adsorbed pyridine on degassed and reduced fresh Pt/ASA catalysts and fresh ASA carrier were recorded (see Fig. 1). The silica–alumina substrate displays both Brønsted and Lewis acid sites. This originates from isomorphous substitution of tetravalent silicon by trivalent aluminium in the silica lattice [17]. As the normally hexacoordinated aluminium atom has been forced to adopt a tetracoordinated structure, aluminum tends to acquire a pair of electrons, thus behaving as a Lewis acid in the absence of water, and as a Brønsted acid in the presence of one water molecule [18]. In this study, the integrated peak intensities at 1450 cm^{-1}, coming from pyridine coordinated on Lewis acid sites, and at 1540 cm^{-1}, attributed to pyridinium ion formed by interaction with Brønsted acid sites [19], were determined. In Table 1 the Brønsted/Lewis ratio is presented (I_{1543}/I_{1452}) for each catalyst and each pretreatment. As it can be observed, degassed Pt/ASA catalyst showed lower Brønsted/Lewis (B/L) ratio as compared to the ASA support. The decrease in B/L acidity ratio for Pt/ASA catalysts might be due to a decrease in the Brønsted acidity brought about by the promoter incorporation [20,21], or due to the fact that Pt-crystallites nucleate at the strong acid sites which are no longer available to bind pyridine [22].

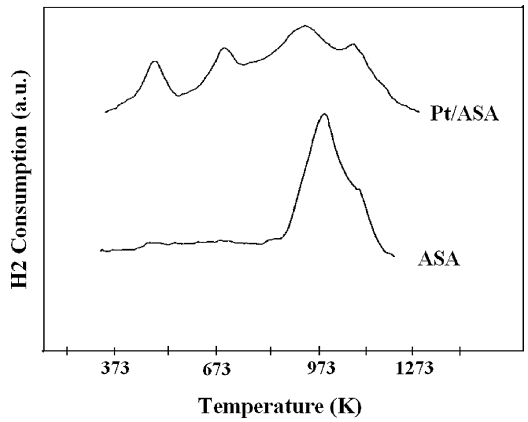

Fig. 2. TPR profiles of fresh catalysts.

Comparing the acidity of degassed and reduced ASA and Pt/ASA (Table 1), it appears that H_2 reduction affected catalysts acidity. Nevertheless, the increase in the B/L acidity ratio was much stronger for Pt/ASA than for ASA. This fact suggests that a H_2 effect is produced by Pt metal phases. In order to investigate this phenomenon a TPR analysis of fresh Pt/ASA and ASA samples was carried out. The TPR profile of ASA support (see Fig. 2) shows a hydrogen consumption peak at about 973 K, with a shoulder on the high temperature side (>973 K), probably due to reduction of impurities on the support [20]. The Pt/ASA TPR profile shows four peaks at 456, 658, 907 and 1059 K. The first one can be assigned to the reduction of Pt^{2+} to Pt^0, while the high temperature peaks can be related again to the reduction of ASA impurities. The peak at 658 K shall be assigned to the H_2 that dissociates on Pt metal sites.

Based on the results of IR spectra of adsorbed pyridine and TPR analysis it seems that H_2 dissociates on Pt metal sites and that the hydrogen atoms formed spillover to the surface of the carrier where they react with Lewis and/or Brønsted sites affecting the acidity. For ASA carrier, the H_2 does not dissociate and thus H_2 does not affect the acidity.

The TPD-NH_3 measurements were carried out to compare the total acidity of Pt/ASA and ASA samples used in the activity tests at 493 K, 20 wt.% glycerol aqueous solution and under H_2 and N_2 pressure with the acidity of the fresh samples. The aim was to determine if the reaction conditions might change the acidity of the support. The ammonia molecule is sufficiently small to enter the pores of the catalysts and to adsorb on Brønsted and Lewis acid sites. The TPD-NH_3 profiles are shown in Fig. 3. The total acidity of the spent and used samples, which was calculated as the sum of the weak, medium and strong acid sites obtained after fitting of the experimental curves by the Gaussian deconvolution (not shown here), is listed in Table 2.

As it can be observed from Table 2, after the reaction in the aqueous phase the concentration of the acid sites strongly increased (2–3 fold). Mostly affected was the concentration of strong acid sites, while the effect on the weaker sites was lesser. The interpretation of this significant increase of strong acid sites during the reaction is not totally clear. It is well known that the SiO_2 and Al_2O_3 surfaces increase their acidity with surface hydration processes [23,24], and it is plausible the spent samples to keep part of the acid sites created through the interaction with water molecules after the pretreating with He.

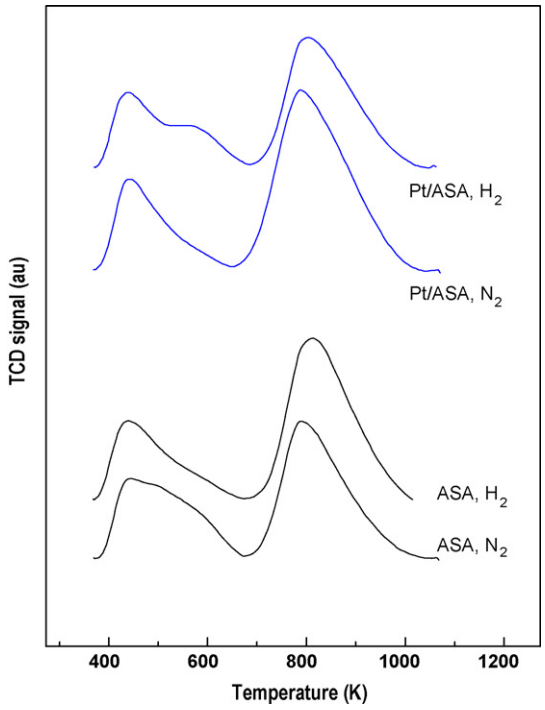

Fig. 3. TPD-NH_3 profiles of spent Pt/ASA and ASA catalysts. (Note: this picture is intended for colour reproduction on the web and black and white in print.)

Spent Pt/ASA and ASA samples showed different acidity regarding they were used with N_2 or H_2 atmosphere. For ASA support, the spent sample used under H_2 presented higher acidity than the spent sample used under N_2, while for Pt/ASA catalyst, the sample used under N_2 atmosphere was the one with the highest acidity. All the samples were tested along the same time under the same operating conditions, therefore differences in total acidity on spent samples should be associated to another effect than water interaction. It seems that some different chemical reactions occurred in the system when Pt was present or when the activity tests were performed under N_2 atmosphere, and that these chemical reactions affected the acidity of the spent samples.

3.2. Surface features of fresh and spent Pt/ASA and ASA catalyst

The chemical species present on the catalysts surfaces and their proportions were evaluated by XPS. Binding energies of core electrons of fresh and spent catalysts are reported in Table 3. The selected samples were the same analyzed by TPD-NH_3 and TGA: Pt/ASA and ASA used in the activity tests with 493 K reaction temperature, 20 wt.% glycerol initial concentration, and under H_2 or N_2 atmosphere.

Table 2
Acid properties of fresh and spent catalysts.

Sample	Amount of acid sites[b] (mmol $NH_3 \cdot g_{cat}^{-1}$)			
	Weak	Medium	Strong	Total
ASA, fresh	1.56 (467 K)	3.19 (554 K)	0.76 (894 K)	5.51
ASA, N_2, 220 °C[a]	1.58 (441 K)	3.59 (528 K)	7.37 (814 K)	12.53
ASA, H_2, 220 °C[a]	1.72 (439 K)	2.32 (515 K)	9.05 (827 K)	13.09
Pt/ASA, fresh	0.82 (459 K)	1.79 (532 K)	1.63 (798 K) 2.60 (884 K)	6.83
Pt/ASA, N_2, 220 °C[a]	1.70 (441 K)	2.16 (506 K)	11.46 (814 K)	15.32
Pt/ASA, H_2, 220 °C[a]	1.99 (441 K)	2.36 (546 K)	7.36 (827 K)	11.71

[a] Catalyst samples used under 493 K reaction temperature, 45 bar pressure, 41 mL 20 wt. % glycerol initial concentration, 166 mg catalyst/mg glycerol and 24 h reaction time.
[b] Amount of desorbed ammonia determined by TPD of NH_3.

The binding energy of Pt $4d_{5/2}$ level for fresh Pt/ASA sample indicates that Pt is present as Pt^0 (315.1 eV) [25]. In the Pt/ASA samples used in the reaction, both under N_2 or H_2, only a slight variation on the Pt $4d_{5/2}$ binding energy was observed, meaning that the Pt remained as Pt^0 during the reaction. Not any other Pt component at higher binding energies that could correspond to oxidized species of Pt was observed. For instance, if PtO_2 species were present a component somewhere around binding energy of 318 eV should be observed [26]. In addition, the C 1s line exhibited three components at 284.9, 286.7 and 288.5 eV. The component at 284.9 eV comes from hydrocarbons contamination. The component at 286.7 eV is related to a C–O bond, while the highest binding energy (288.5 eV) is associated to COO groups.

From XPS peaks intensities, atomic surface ratios were computed and the results are presented in Table 4. For both Pt/ASA and ASA catalysts, the C/Al surface atomic ratio was higher in the samples used in reaction as compared to fresh samples, and this increment is associated to coke formation. Similar C/Al ratios were measured for the samples run in H_2 and N_2, therefore it seems that under the experimental conditions coke formation was unaffected by the reacting atmosphere. For Pt/ASA catalyst, Pt/Al surface ratio suffered more than one third decrease in the samples used in reaction under H_2 or N_2 pressure. This effect might be related to the covering of Pt particles by coke deposits. Taking into account the mil operating conditions (493 K) it does not seem plausible a decrease on the Pt/Al surface ratio caused by Pt particles siterization.

3.3. Activity test results

In order to be able to establish the role played by the metallic (Pt) and acid sites of the support in the hydrogenolysis and further degradation of glycerol, experiments with Pt/ASA catalyst and ASA support were carried out with 20 wt.% glycerol initial concentration and under H_2 or N_2 pressure. The main products observed in liquid phase were: 1,2-PDO, 1,3-PDO, 1-propanol (1-PO), 2-propanol (2-PO), acetol, propanal, acetone, acrolein, propanoic acid, ethylene glycol, methanol, ethanol, acetaldehyde and acetic acid. The following products were also detected in some experiments: n-hexanone, propyl propionate, 2,5-hexanedione, 2-hydroxi-3-hexanone. Methane, ethane, ethylene and propene were detected in the gas phase, with trace amounts of volatile compounds (acetaldehyde, propanal, acrolein, and acetone).

For an easier interpretation of the results, liquid products were divided in three groups: *hydrogenolysis products*: (C3) 1,2-PDO, 1,3-PDO, *n*-PO, acetol, propanal, acetone, acrolein and propionic acid. *Cracked products*: (C < 3) ethylene glycol, methanol, ethanol, acetaldehyde and acetic acid. *Addittion products*: (C > 3) n-hexanone, propyl propionate, 2,5-hexanodione, 2-hydroxi-3-hexanone. In Fig. 5 a proposal for 1,2-PDO and 1,3-PDO formation and consumption is presented. Glycerol is first dehydrated to acetol, which is hydrogenated to 1,2-PDO. 1,2-PDO is further dehydrated to acetone and propanal; after the hydrogenation of these products 1-PO and 2-PO are formed. Previous published works proved that 1,3-PDO comes from the hydrogenation of 3-HPA [13], and that acrolein is formed after the dehydration of 3-HPA [27]. Based on the scheme, hydrogenolysis products can be divided at the same time in: *dehydrated products*: acetol, propanal, acetone and acrolein, and in *hydrogenated products*: 1,2-PDO, 1,3-PDO and *n*-PO. Glycerol conversion and selectivity values for each experiment are presented in Table 5.

The first important feature to be analyzed is that in the experiments with Pt/ASA and under N_2 pressure glycerol hydrogenolysis occurred. Moreover, in the activity test done with Pt/ASA, 493 K and N_2 pressure, glycerol conversion and selectivity values to 1,2-PDO

Table 3
Binding energies (eV) of core electrons of Al 2p, Si 2p, O 1s, C 1s and Pt $4d_{5/2}$ in fresh and used catalysts.

Catalyst	Al 2p	Si 2p	O 1s	C 1s (%)	Pt $4d_{5/2}$	
ASA	Fresh	74.5	102.9	532.6	286.6 (71) 288.5 (28)	-
	Used in reaction under N_2 and 493 K	74.7	103.0	532.7	286.7 (66) 288.7 (34)	-
	Used in reaction under H_2 and 493 K	74.6	103.0	532.8	286.5 (64) 288.7 (36)	-
Pt/ASA	Fresh	74.6	103.0	532.7	286.6 (66) 288.5 (34)	315.1
	Used in reaction under N_2 and 493 K	74.7	102.9	532.8	286.7 (71) 288.7 (29)	314.9
	Used in reaction under H_2 and 493 K	74.6	102.9	532.9	286.8 (66) 288.5 (34)	314.9

Table 4
Surface atomic ratios obtained by XPS in fresh and used catalysts.

Catalyst	Si/Al	O/Al	C/Al	Pt/Al	
ASA	Fresh	0.83	4.78	0.14	–
	Used in reaction under N_2 and 493 K	0.78	4.66	0.97	–
	Used in reaction under H_2 and 493 K.	0.79	4.71	0.85	–
Pt/ASA	Fresh	0.84	4.83	0.12	0.003
	Used in reaction under N_2 and 493 K	0.78	4.58	0.89	0.002
	Used in reaction under H_2 and 493 K	0.66	4.14	0.82	0.002

Table 5
Glycerol conversion and selectivity values after 24 h reaction time as a function of the reaction temperature, the catalyst utilized, and the reacting atmosphere. 41 mL 20 wt.% glycerol initial concentration, 45 bar pressure, 166 mg catalyst/mg glycerol and 550 rpm.

Catal.	Atmo	Temp. (K)	Conv[a] (%)	Conv[b] (%)	Selectivity (%)						Ratio[e] Hyd/Dehydr
					1,2-PDO	1,3-PDO	Acetol	1PO+2PO	Propanal	Others	
Pt/ASA	H_2	493	19.0	19.8	31.9	4.5	1.2	53.8	0.3	8.3[c]	36.7
ASA	H_2	493	2.6	3.4	2.0	<0.0	12.6	23.2	38.2	24.0[d]	0.5
Pt/ASA	H_2	513	87.6	90.0	11.2	0.7	4.2	59.7	1.2	23.0[c]	11.5
ASA	H_2	513	9.5	10.0	0.4	<0.0	6.7	13.5	31.2	48.2[d]	0.5
Pt/ASA	N_2	493	22.7	26.6	35.3	1.2	15.5	22.6	1.0	24.4[c]	3.0
ASA	N_2	493	1.9	2.4	1.7	<0.0	11.2	7.7	25.7	54.0[d]	0.2
Pt/ASA	N_2	513	34.8	45.6	6.8	1.3	5.3	40.4	1.1	45.1[c]	4.0
ASA	N_2	513	6.2	6.6	3.0	<0.0	6.0	3.8	11.8	75.4[d]	0.4

[a] Glycerol conversion = sum of C-based mol of all detected liquid products/initial C-based mol of glycerol.
[b] Glycerol conversion = (glycerol $t = 0$ – glycerol $t = 24$ h)/glycerol $t = 0$).
[c] Acetaldehyde, acetone, methanol, ethanol, ethylene glycol, acetic acid, propanoic acid and addition products.
[d] Acetaldehyde, acetone, acrolein, ethanol, propanoic acid and addition products.
[e] Ratio between hydrogenated products (1,2-PDO, 1,3-PDO and n-propanol) and dehydrated products (acetol, propanal, acetone and acrolein).

were found to be slightly higher to those obtained with the same operation condition but under H_2 pressure (see Table 5). The analysis of the gas phase revealed the presence of small amounts of H_2 and CO_2. Therefore, hydrogen was formed during the process and part of it was consumed in the hydrogenation reactions. Hydrogen production from glycerol through aqueous phase reforming (APR) is a well-known process [28].

$$C_3H_5(OH)_3 + 3H_2O \rightarrow 3CO_2 + 7H_2$$

It is reported that Pt-based catalysts show good performance for the glycerol APR reactions [29], hence, although the reaction conditions (493 K and 45 bar) are not the optimum conditions for the process [30], it is plausible that small amounts of H_2 were formed through glycerol APR. No CO was detected in the gas phase, which can be explained by the high water/carbon ratio under the reaction conditions used, causing a promotion of the water gas shift reaction [31]:

$$CO + H_2O \leftrightarrow H_2 + CO_2$$

In the activity tests performed with Pt/ASA under H_2 pressure or with ASA (both under H_2 or N_2 pressure) nor CO_2 neither CO was detected when analyzing the gas phase. It seems that no significant APR reactions occurred with Pt/ASA under hydrogen pressure or when ASA support was used alone. The inhibiting effect of hydrogen on the reforming rate has already been reported to be caused by the blocking of surface sites by adsorbed hydrogen atoms and by decreasing the surface concentrations of reactive intermediates formed from dehydrogenation reactions [30].

Due to the specific characteristics of the reacting system (it was not a close system as N_2 entered from the flowing line when the pressure decreased in the reactor, and gas from the reactor went out into the flowing line when the pressure increased), it was not possible to measure the amount of H_2 and CO_2 formed by glycerol APR. Nevertheless, a comparison between the glycerol conversion values obtained by mass balance and glycerol conversion values obtained with the formula describe in Section 2.2 gives a qualitative idea of the amount of gas products formed. As it can be observed in Table 5, in the activity tests with Pt/ASA and under H_2 atmosphere both glycerol conversion values are in good agreement, and the slightly higher values achieved with the mass balance based method can be assigned to the error of the analysis procedure and to the formation of gas products (methane, ethane and propane). Nonetheless, in the tests with Pt/ASA but under N_2 atmosphere the differences between both conversion values are more significant, suggesting a higher formation of gas products. Due to the fact that

Table 6
Yield values after 24 h reaction time for different groups of compounds as a function of the catalyst and the reacting atmosphere.

Catal.	Atmos.	Temp. (K)	Yield		
			Hydrog.[a]	Crack.[b]	Addit.[c]
Pt/ASA	H_2	493	17.61	1.18	0.18
ASA	H_2	493	2.06	0.06	0.50
Pt/ASA	H_2	513	72.18	12.44	2.98
ASA	H_2	513	5.23	0.10	4.18
Pt/ASA	N_2	493	18.63	3.50	0.57
ASA	N_2	493	1.16	0.15	0.59
Pt/ASA	N_2	513	24.85	9.22	0.73
ASA	N_2	513	2.52	0.95	2.73

[a] Hydrogenolysis products: 1,2-PDO, 1,3-PDO, 1-PO, 2-PO, acetol, propanal, acetone, acrolein and propionic acid.
[b] Cracked products: ethylene glycol, methanol, ethanol, acetaldehyde and acetic acid.
[c] Addition products: n-hexanone, propyl propionate, 2,5-hexanodione, 2-hydroxi-3- hexanone.

glycerol APR was not observed in the experiments under H_2 pressure, we can assigned the increase in gas products formation in the activity tests under N_2 pressure to the H_2 and CO_2 formed through glycerol APR.

Next the results obtained with ASA and Pt/ASA, when using the same operation conditions, are compared. In the experiments with ASA support, dehydrated products were dominant, while in the experiments with Pt/ASA major product came from hydrogenation reactions (see hydrogenated/dehydrated products ratio in Table 5). These data confirm that the acid sites of the ASA support are responsible for dehydration reactions [32] while Pt metal sites catalyze hydrogenation reactions. The yield to acetol and to products derived from acetol (PDOs, propanal, acetone, and *n*-PO) was higher in the experiments with Pt/ASA than with ASA. Hence, when Pt was present, the quantity of acetol formed from glycerol (formed and reacted) was bigger, suggesting that Pt sites are also involved on glycerol dehydration to acetol. This also explains the considerable higher conversions achieved with Pt/ASA.

In the experiments with Pt/ASA the yield to cracked products was significantly higher than in the experiments with ASA (Table 6). It is well known that Pt facilitates C–C bond cleavage when it interacts with acidic supports [33]. On the other hand, the yield to addition products was higher in the experiments with ASA. It seems that Pt makes the formation of addition products more difficult through the stabilization of possible building blocks. Coke formation measurements done by TGA analysis of spent Pt/ASA and ASA samples are not very conclusive due to the small differences in observed values (see Fig. 4). Nevertheless it seems that in the experiments at 493 K, less coke was formed with Pt/ASA than with ASA (under N_2 and H_2) even though higher conversion values were achieved with Pt/ASA. The presence of Pt metal sites could reduce the proportion of precursors that lead to coke formation. In the study of benzene alkylation with pure propane using Ga–Pt modified ZSM-5 catalysts, Todorova et al. observed that the presence of Pt reduced coke formation [34]. They proposed that Pt has a role of the entrance for hydrogen spillover which moderates coke formation.

When comparing the reacting atmosphere, the effect of N_2 instead of H_2 atmosphere on glycerol conversion appears contradictory. With ASA catalyst, glycerol conversion values were lower when N_2 was utilized instead of H_2, for both 493 and 513 K reaction temperatures. However, with Pt/ASA, glycerol conversion with N_2 was lower at 513 K, compared to that obtained under H_2 pressure, but slightly higher at 493 K (see Table 5).

Hydrogen availability might be the factor explaining this behaviour. In the activity tests under H_2 pressure, this reactant needs to dissolve from the gas phase to the aqueous solution, to diffuse from the bulk fluid to the external surface of the catalyst and from the external surface to the interior of the pores, and finally to adsorb on the active sites. As it has been pointed out before, no significant APR occurred in the activity tests with Pt/ASA under H_2 pressure or in the activity tests where ASA support was used, and therefore all the H_2 available in those activity tests came from the dissolved H_2. In the activity tests with Pt/ASA under N_2 pressure, H_2 was formed by APR of glycerol on Pt sites [33] and hence, this H_2 can react easily with molecules adsorbed on adjacent Pt sites, or, after spill over, with molecules adsorbed on acid sites of the ASA support. In the activity tests with ASA support, no significant H_2 was formed through APR. Hence, for both reacting temperatures (493 and 513 K), there was lower hydrogen availability in the activity tests under N_2 pressure and as a result lower glycerol conversions were achieved as compared to the tests under H_2 pressure. For Pt/ASA catalyst, similar glycerol conversion values were achieved in the activity tests at 493 K under N_2 or H_2 pressure. It seems that in both activity tests there was a similar concentration of H_2 molecules near the active sites of the catalyst: due to H_2 formed through glycerol APR under N_2 pressure and due to diffusion of dissolved H_2 under H_2 pressure. At 513 K, however, glycerol conversion increased greatly in the activity test under H_2 pressure (87.6%), while under N_2 pressure the increased was not that marked (34.8%). It seems that at 513 K the concentration of H_2 molecules close to the active sites was higher in the activity test under H_2 pressure than in the activity test under N_2 pressure. This can be explained considering the effect of the temperature on H_2 solubility.

A thermodynamic analysis was performed to determine the influence of temperature on hydrogen solubility. Due to the nature of the components and the high working pressures, Peng–Robinson method was selected. The first step was to validate the selected method, comparing the values for the Henry's constant (K_H) estimated and the values reported in the literature. In 1997 Eklund et al. [35] measured Henry's constant for hydrogen in high subcritical and supercritical aqueous systems, using $Hg|HgO|ZrO_2(Y_2O_3)|NaOH(aq)|H_2(Pt)$ cell at 275 bar and different temperatures. In Table 7 a comparison between the values reported and the values obtained in the thermodynamic analysis at the same pressure and temperature conditions, and pure water/hydrogen system, are presented. Experimental values and the ones obtained through the simulation are in a good agreement, thus the selected method can be used for further analysis. The effect of temperature in hydrogen solubility for a 45 bar hydrogen pressure and 20 wt.% glycerol water system is also presented in Table 7.

As it can be observed, H_2 solubility increased around 18% from 493 to 513 K at 45 bar pressure. This increment in H_2 solubility and the increase in the reaction kinetics seem to be the reason for the higher conversions achieved with Pt/ASA under H_2 atmosphere. Under N_2 pressure and 513 K the concentration of H_2 molecules (formed by glycerol APR) near the active sites seems that it was not as high as the existing in the activity test under H_2 pressure and therefore lower glycerol conversion was obtained.

It has been suggested that increasing H_2 availability increases glycerol conversion, and as it can be observed in Table 6, also the yield to hydrogenolysis products. Nonetheless, as it is presented in Fig. 5, the first step in the formation of hydrogenolysis products is always a dehydration step. The enhanced glycerol conversion to dehydrated products could be assigned to the higher desorption rates for adsorbed dehydrated products, mainly acetol, in the presence of H_2.

Operating with high reacting temperatures and pressures increases hydrogen solubility in glycerol/water liquid solutions. High glycerol conversion (87.6%) was achieved in the activity test with Pt/ASA, 513 K and H_2 atmosphere. Nonetheless, the selectivity to 1,2-PDO (11.2%) is far from the best results cited in literature for

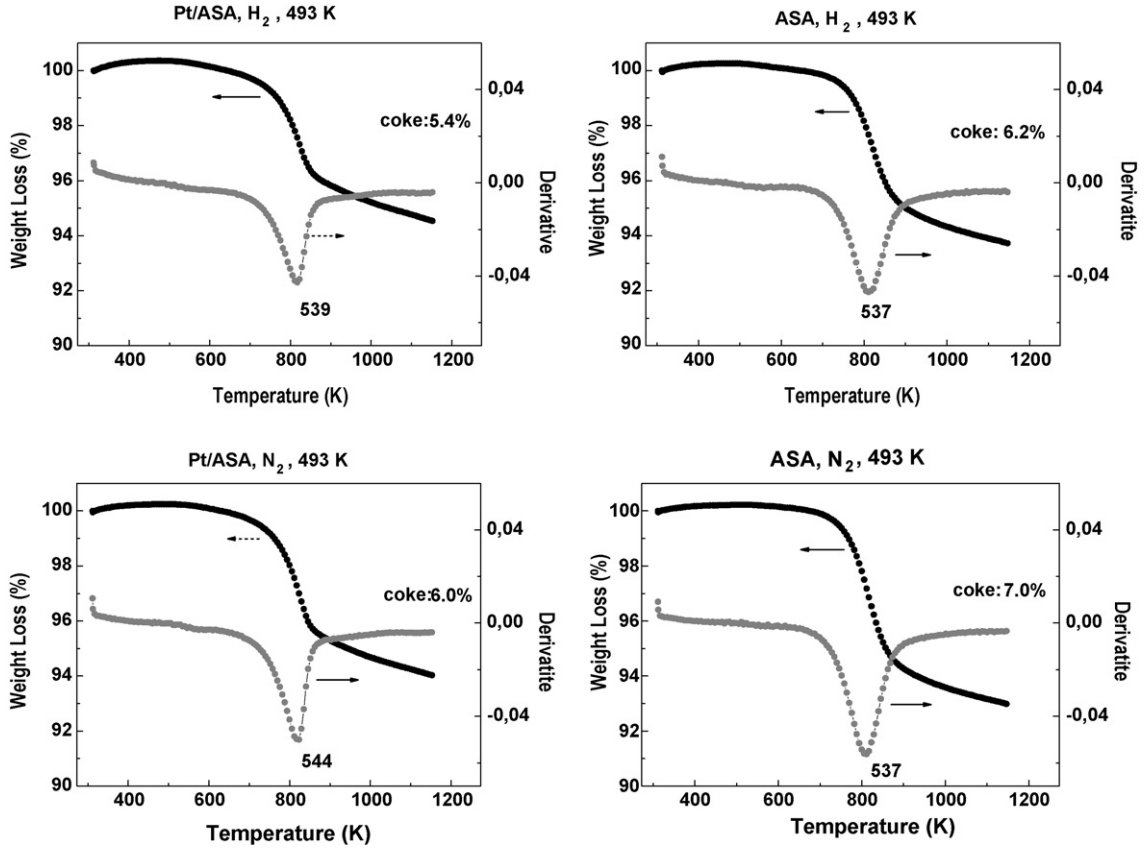

Fig. 4. Evolution of weight loss (black) and DP/DT (grey) with the temperature for Pt/ASA and ASA catalysts after 24 h reaction time. Operating Conditions: 493 K, 20 wt.% glycerol initial concentration, 45 bar H_2 or N_2 pressure.

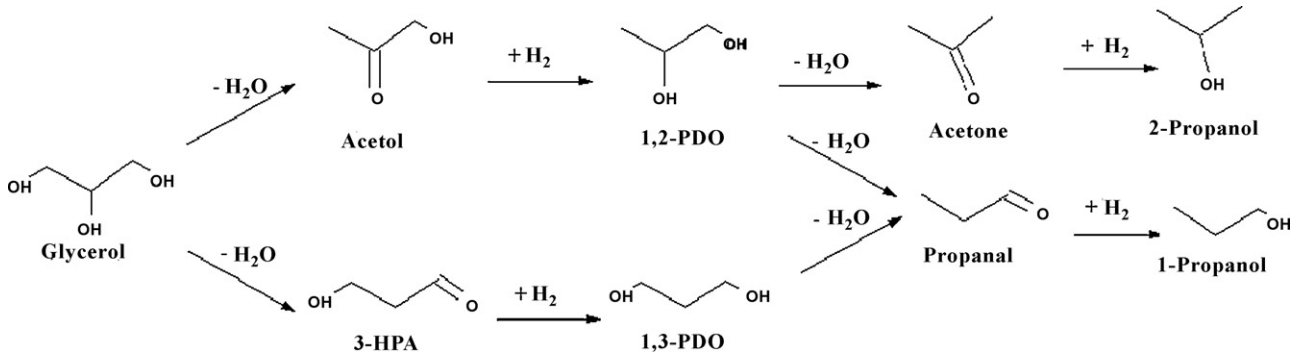

Fig. 5. Proposal for PDOs formation and further hydrogenolysis products from glycerol.

vapour phase glycerol hydrogenolysis [11] or for a two-step process [2] (>90% yield to 1,2-PDO). However these processes imply higher processing costs due to higher energy consumption and higher equipment dimensions as compared to liquid phase processes. The main reason for the low selectivity to 1,2-PDO obtained is that increasing reaction temperature favours a higher H_2 solubility but also the formation of cracking products (see Table 6) and 1,2-PDO further hydrogenolysis to 1-PO and 2-PO (see Table 5). Hence, it is not convenient to operate at high temperatures. Hydrogen formed through glycerol APR showed to be effective to react with glycerol and intermediate molecules. This opens an interesting new field, to research new reacting systems, like the addition

Table 7
A comparison between reported experimental values for K_H [35] and values for K_H obtained in the thermodynamic analysis for pure water system, and K_H and H_2 concentration values obtained in the thermodynamic analysis for 20 wt. % glycerol/water system.

Temp. (K)	Solution	K_H (exp.) (mol kg^{-1} bar^{-1})	K_H (therm.) (mol kg^{-1} bar^{-1})
523	Pure water	7.4×10^{-4}	7.9×10^{-4}
573	Pure water	1.7×10^{-3}	1.3×10^{-3}
Temp. (K)	Solution	K_H (exp.) (mol kg^{-1} bar^{-1})	H_2 conc. 45 bar (mol kg^{-1})
493	20 wt.% glycerol/water	6.4×10^{-4}	0.029
513	20 wt.% glycerol/water	7.8×10^{-4}	0.035

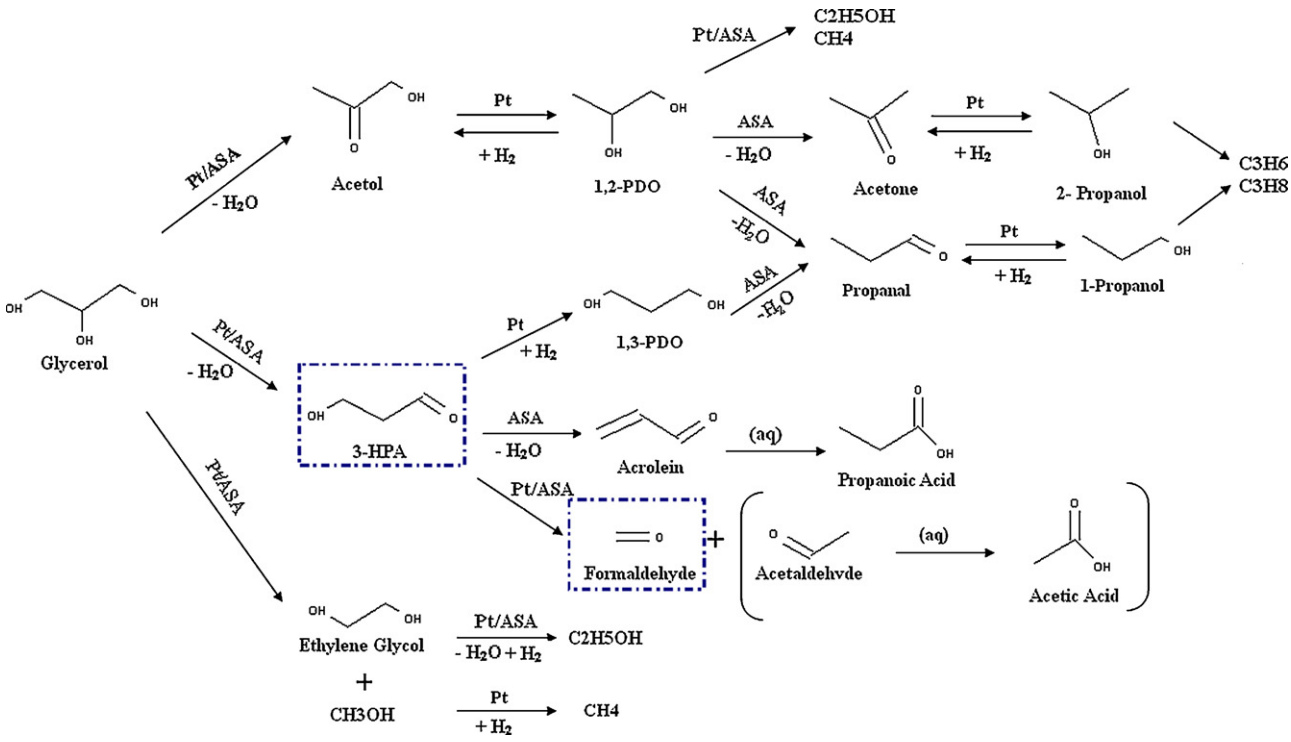

Fig. 6. Reaction scheme of glycerol hydrogenolysis and degradation reactions.

of hydrogen donor molecules, that produce the hydrogen directly in the active sites of the catalyst, allowing working in liquid phase but with moderate temperatures and pressures.

3.4. Reaction mechanism of glycerol hydrogenolysis and degradation over Pt/ASA

Activity tests of some reaction products (acetol, 1,2-PDO, 1,3-PDO, ethylene glycol, and 2-PO) over Pt/ASA were carried out under similar conditions as the ones used for glycerol to elucidate the reaction routes of the products. Conversion and selectivity results of each experiment can be seen in Table 8. In Table 9 detected products for each reactant are listed.

Formation paths of detected hydrogenolysis products (1,2-PDO, 1,3-PDO, 1-PO, 2-PO, acetol, propanal, acetone, acrolein and propionic acid) will be firstly discussed. In the literature it is presented that in the PDOs production process glycerol is first dehydrated to acetol and 3-HPA, which are subsequently hydrogenated to 1,2 and 1,3-PDO, respectively. 3-HPA was not detected in any of the experiments, and it was not found any reference in the literature where this compound was detected. Nimlos et al. reported quantum mechanics calculations in the reaction of glycerol and investigated the dehydration mechanism of protonated glycerol [36]. On the basis of these calculations, Tsukuda et al. speculated on probable routes for glycerol dehydration [27]. When protonation occurs at the secondary hydroxyl group of glycerol, a water molecule and a proton are eliminated from the protonated glycerol, and then 3-HPA is produced by tautomerism. 3-HPA is readily dehydrated into acrolein or hydrogenated to 1,3-PDO. When protonation proceeds at a terminal hydroxyl group, acetol is produced. Since the stability of 3-HPA and acetol are different, stable acetol can be detected in the reaction while unstable 3-HPA is nearly instantaneously converted in subsequent reactions. Several works suggest that propanoic acid is produced through the oxidation of acrolein in aqueous solution [10,27]. Moreover, Gyorffy et al. studying acrolein hydrogenation on PdPt catalyst revealed that the formation of propanal by C=C bond hydrogenation was the main reaction [37]. Propanal and acetone are formed from PDOs dehydration reactions, and these molecules are subsequently hydrogenated to 1-PO and 2-PO, respectively. Thus, there are two consecutive hydrogenolysis reactions:

$$\text{Glycerol} \rightarrow \text{Acetol} \rightarrow \text{1, 2-PDO} \rightarrow \text{propanal, acetone} \rightarrow n\text{-PO}$$

1,2-PDO and 1,3-PDO showed similar reactivity (see Table 8). This result differs from the study presented by Miyazawa et al. in which 1,3-PDO was much more reactive than 1,2-PDO on Ru/C + amberlyst catalyst [5]. However, Lehr et al., investigating PDOs dehydration to propanal in sub and supercritical water with the addition of bivalent transition metals, observed that 1,3-PDO was less reactive than 1,2-PDO [38]. These results suggest that the

Table 8
Results of the reaction of various compounds after 24 h reaction time.

Reactant	Initial conc. (wt.%)	Conv.[a] (%)	Selectivity to liquid products							
			1,2-PDO	1,3-PDO	Acetol	1PO + 2PO	EG	Ethanol	Acetone	Propanal
Acetol	4.2	100	76.1	0.0	–	19.6	0.0	1.1	0.8	1.9
1,2-PDO	3.8	12.9	–	0.0	3.6	92.9	0.0	2.4	0.5	0.6
1,3-PDO	3.8	10.5	0.0	–	0.0	98.0	0.0	1.6	0.0	0.4
EG	1.6	1.9	0.0	0.0	0.0	0.0	–	100	0.0	0.0
2-PO	2.6	56.3	0.0	0.0	0.0	–	0.0	0.0	100	0.0

[a] Reaction conditions: 493 K reaction temperature, 45 bar H_2 pressure, 550 rpm and 166 mg Pt/ASA/mg reactant.

Table 9
Detected products for each experiment.

Reactant	Detected products
Acetol	Propanal, acetone, 1,2-PDO, 1,3-PDO, 1-PO, 2-PO, ethanol, 2,5-hexanedione, ethane and propane
1,2-PDO	Propanal, acetone, 1-PO, 2-PO, ethanol, acetol, ethane, and propane
1,3-PDO	Propanal, ethanol, 1-PO, ethane, and propane
EG	Ethanol
2-PO	Acetone, propene and propane

relative reactivity between 1,2-PDO and 1,3-PDO is highly dependent on the operations conditions and on the catalytic system used. In the activity test with 1,2-PDO as reactant, acetol was detected, while in the reaction of 2-PO, acetone was the main product, indicating reversible cetone/alcohol hydrogenation/dehydrogenation reactions.

Next, the route to cracked products is considered. The cracked products detected were: ethylene glycol, methanol, ethanol, acetaldehyde and acetic acid. In the case of the reaction of glycerol, ethylene glycol and methanol were obtained. However, they were not detected in the experiments with 1,2-PDO, 1,3-PDO, acetol or 2-PO as reactants, suggesting that ethylene glycol and methanol are formed directly from glycerol. Furthermore, the conversion of ethylene glycol was low when this compound was used as a reactant (Table 8). This finding explains why ethylene glycol was observed in the reaction of glycerol. Ethanol can be formed during hydrogenolysis of ethylene glycol. Ethanol and methane were also obtained in the activity tests starting with 1,2-PDO and 1,3-PDO but not in the activity test starting with 2-PO, therefore, ethanol and methane are formed from PDOs. Tsukuda et al proposed that acetaldehyde and formaldehyde are formed from 3-HPA, and that acetaldehyde is afterwards oxidized to acetic acid [27]. Finally, gas products observed were methane, ethylene and propane. Methane can be formed from methanol hydrogenation and from PDOs degradation, while ethylene and propane might come from ethanol and *n*-PO dehydration respectively.

A proposal for glycerol hydrogenolysis and degradation reactions, which takes into account all the information obtained from the experimental data and the current body of work in this area, is presented in Fig. 6. 3-HPA and formaldehyde are surrounded by a dotted line as they were not detected in any experiment.

4. Conclusions

The role of acid and metal sites of Pt/ASA was studied in the glycerol hydrogenolysis process to obtain 1,2-PDO. ASA acid sites are responsible for glycerol dehydration to acetol while Pt metal sites catalyze acetol hydrogenation to 1,2-PDO. However, the amount of acetol formed and reacted was higher with Pt/ASA than with ASA, suggesting that Pt sites are involved on glycerol dehydration to acetol. Pt also catalyzes C–C bond cleavage, and its presence reduces the formation of coke, as Pt is responsible of the entrance for hydrogen spillover which moderates coke formation.

Hydrogen availability seems to have a direct effect on glycerol conversion. In the experiments with Pt/ASA and under N_2 pressure, glycerol hydrogenolysis took place due to the H_2 available from the aqueous phase reforming of glycerol. At 493 K, the H_2 formed in the Pt sites through glycerol APR in the activity test under N_2 pressure seems to be as effective as the H_2 dissolved in the aqueous phase from the gas hydrogen phase and diffused to the catalysts.

Low selectivity values to 1,2 and 1,3-PDO were achieved as compared to other results published in the literature. The fact that Pt/ASA catalyzes C-C bond cleavage and PDOs further hydrogenolysis to 1-PO is the main reason that reduces process selectivity to desired products.

Acknowledgments

This work was supported by funds from the Ministerio de Ciencia e Innovación ENE2009-12743-C04-04, and from the Gobierno Vasco (Programa de Formación de Personal Investigador del Departamento de Educación, Universidades e Investigación). The authors also gratefully acknowledge Shell for providing the Pt/ASA catalyst and the University of the Basque Country and the Institute of Catalysis and Petrochemistry of Madrid for their technical support.

References

[1] M. Pagliaro, M. Rossi, The Future of Glycerol: New Usages for a Versatile Raw Material, 1st ed., RSC Publishing, Cambridge, 2008.
[2] C. Chiu, L.G. Schumacher, G.J. Suppes, Biomass Bioenergy 27 (2004) 485–491.
[3] A. Corma, S. Iborra, A. Velty, Chem. Rev. 107 (2007) 2411–2502.
[4] S. Shelley, Chem. Eng. Prog. 103 (2007) 7–11.
[5] T. Miyazawa, Y. Kusunoki, K. Kunimori, K. Tomishige, J. Catal. 240 (2006) 213–221.
[6] T. Kurosaka, H. Maruyama, I. Naribayashi, Y. Sasaki, Catal. Commun. 9 (2008) 1360–1363.
[7] J. Feng, H. Fu, J. Wang, R. Li, H. Chen, X. Li, Catal. Commun. 9 (2008) 1458–1464.
[8] L. Ma, D. He, Z. Li, Catal. Commun. 9 (2008) 2489–2495.
[9] J. Chaminand, L. Djakovitch, P. Gallezot, P. Marion, C. Pinel, C. Rosier, Green Chem. 6 (2004) 359–361.
[10] S. Sato, M. Akiyama, R. Takahashi, T. Hara, K. Inui, M. Yokota, Appl. Catal. A: Gen. 347 (2008) 186–191.
[11] M. Akiyama, S. Sato, R. Takahashi, K. Inui, M. Yokota, Appl. Catal. A: Gen. 371 (2009) 60–66.
[12] Y. Kusunoki, T. Miyazawa, K. Kunimori, K. Tomishige, Catal. Commun. 6 (2005) 645–649.
[13] T. Miyazawa, S. Koso, K. Kunimori, K. Tomishige, Appl. Catal. A: Gen. 318 (2007) 244–251.
[14] T. Miyazawa, S. Koso, K. Kunimori, K. Tomishige, Appl. Catal. A: Gen. 329 (2007) 30–35.
[15] J.Z. Shyu, K. Otto, Appl. Surf. Sci. 32 (1988) 246–252.
[16] C.D. Wagner, W.M. Riggs, L.E. Davis, J.F. Moulder, G.E. Muilenberg, Handbook of X-ray Photoelectron Spectroscopy, 1st ed., Perkin Elmer Co., Eden Pairie, MN, 1979.
[17] P. Berteau1, B. Delmon, J.-L. Dallons, A. Van Gysel, Appl. Catal. 70 (1991) 307–323.
[18] K. Tanabe, Solid Acids and Bases, 1st ed., Academic Press, New York, 1970.
[19] E.P. Parry, J. Catal. 2 (1963) 371–379.
[20] R Navarro, B. Pawelec, J.L.G. Fierro, P.T. Vasudevan, Appl. Catal. A: Gen. 148 (1996) 23–40.
[21] N.Y. Topsoe, H. Topsoe, J. Catal. 139 (1993) 641–651.
[22] S. Jaenicke, G. Khuan Chuah, P. Zhan, in: Hideshi Hattori, Kiyoshi Otsuka (Eds.), Studies in Surface Science and Catalysis, Elsevier, 1999, pp. 165–170.
[23] C.H. Sun, J.C. Berg, J. Chromatogr. A 969 (2002) 59–72.
[24] M Templer, D. Chvedov, Langmuir 18 (2002) 7936–7942.
[25] G. Corro, J.L.G. Fierro, V.C. Odilon, Catal. Commun. 4 (2003) 371–376.
[26] L. Guczi, A. Sarkany, Z. Koppany, Appl. Catal. A: Gen. 120 (1994) L1–L5.
[27] E. Tsukuda, S. Sato, R. Takahashi, T. Sodesawa, Catal. Commun. 8 (2007) 1349–1353.
[28] R.D. Cortright, R.R. Davda, J.A. Dumesic, Nature 418 (2002).
[29] R.R. Davda, J.W. Shabaker, G.W. Huber, R.D. Cortright, J.A. Dumesic, Appl. Catal. B: Environ. 43 (2003) 13–26.
[30] J.W. Shabaker, R.R. Davda, G.W. Huber, R.D. Cortright, J.A. Dumesic, J. Catal. 215 (2003) 344–352.
[31] N. Luo, X. Fu, F. Cao, T. Xiao, P.P. Edwards, Fuel 87 (2008) 3483–3489.
[32] G.M. Kramer, G.B. McVicker, J.J. Ziemiak, J. Catal. 92 (1985) 355–363.
[33] G.W Huber, R.D. Cortright, J.A. Dumesic, Angew. Chem.-Int. Ed. 43 (2004) 1549–1551.
[34] S. Todorova, B. Su, Catal. Today 93–95 (2004) 417–424.
[35] K. Eklund, S.N. Lvov, D.D. Macdonald, J. Electroanal. Chem. 437 (1997) 99–110.
[36] R.M. Nimlos, S.J. Blanksby, X. Qian, M.E. Himmel, D.K. Johnson, J. Phys. Chem. A. 110 (2006) 6145–6156.
[37] N. Győrffy, Z. Paál, J. Mol. Catal. A: Chem. 295 (2008) 24–28.
[38] V. Lehr, M. Sarlea, L. Ott, H. Vogel, Catal. Today 121 (2007) 121–129.